Equilibrium Theory for Complete Adiabatic Adsorption Cycles

Complete adiabatic fixed-bed adsorption cycles with adsorption, heating, and cooling steps are analyzed using simple wave theory. Solutions consist of simple waves, shocks, combined waves, and wave interactions with patterns established by a mapping between hodograph and physical planes. The system considered is benzene adsorbed on activated carbon with nitrogen as the carrier gas.

M.M. Davis and M.D. LeVan
Department of Chemical Engineering
University of Virginia
Charlottesville, VA 22901

Introduction

Vapor phase adsorption processes for recovery of solvents and removal of impurities of moderate volatility frequently utilize hot purge gas regeneration as part of cycles with three steps (adsorption, heating, cooling) or two steps (adsorption, heating). The heating step is generally carried out by passing the hot gas through the bed in the direction opposite to that of the feed for the adsorption step. If solute-free gas is available for cooling it is passed into the bed in the same direction as for heating; otherwise, the cool gas is passed into the bed in the direction for adsorption and deposits some adsorbate in the bed near the inlet. In some instances, when hot effluent will not disrupt a process, the cooling step may be omitted entirely.

The improvement of design methods for fixed-bed adsorption systems depends to a large extent on the development of reliable mathematical models that can be used to predict the performance of a bed during an entire cycle. Energy requirements for beds regenerated thermally can be large and significantly affect the operating cost of an adsorption system. From an economic standpoint, because of the very favorable equilibrium exhibited by modern adsorbents, complete regeneration is not practical and a heel of undesorbed solute is left in the bed after reverse flow heating. The determination of optimal operating conditions involves an assessment of the desirable extent of this heel. A need therefore exists to improve our understanding of the full cyclic behavior of adsorption beds with the long-range goal of improving design methods; it is to this objective that this paper is directed.

Dating back to the early 1940's, the equilibrium theory is the classical method for analysis of fixed-bed sorption operations. While it is clearly deficient in some respects (notably in the neglect of transfer resistances), the equilibrium theory gives an exact solution to hyperbolic conservation laws, clearly showing the wave character of the process and setting an upper limit on the attainable performance of a system. The equilibrium theory has been used to analyze isothermal sorption cycles and cycle steps with nonconstant initial or entry conditions and Langmuir isotherms. For example, see Rhee et al. (1970a), Helfferich and Klein (1970), Grevillot et al. (1974), Bailly and Tondeur (1981), Rhee and Amundson (1982), and Klein et al. (1984).

Previous applications of the equilibrium theory to adiabatic adsorption have been concerned with cycle steps with constant initial and entry conditions (Amundson et al. 1965; Rhee and Amundson, 1970; Rhee et al., 1970b; Pan and Basmadjian, 1970, 1971; Basmadjian et al., 1975; Jacob and Tondeur, 1981, 1983; Friday and LeVan, 1984). Complete cycles and cycle steps with nonconstant initial or entry conditions have not been treated except for liquid phase applications such as the recuperative mode of parametric pumping and the traveling-wave mode of cycling zone adsorption. For these the energy balance can be solved separately, as in Knaebel and Pigford (1983), since thermal effects are associated solely with a change in feed temperature rather than also the result of adsorption.

In this paper we analyze full adiabatic adsorption cycles for single-component adsorption using equilibrium theory. This is the first such treatment of full adiabatic cycles with cycle steps having nonconstant initial conditions. The method adopted is amenable to the use of general adsorption equilibrium relations. We rely extensively on simple wave theory (Courant and Friedrichs, 1948; Lax, 1954, 1957; Jeffrey and Taniuti, 1964; Aris and Amundson, 1973; Jeffrey, 1976) and on the theory of multicomponent chromatography as advanced by Rhee et al. (1970a) and Rhee and Amundson (1982), which establishes the basis for our work. Three cases are considered with benzene adsorbed from nitrogen on activated carbon in two- and three-step cycles.

We obtain results that depend on cyclic operation and would not be revealed by analyses of single cycle steps with constant initial conditions. Regardless of flow direction and whether the

Correspondence concerning this paper should be addressed to M.D. LeVan.

bed is cooled in a separate step of a three-step cycle or at the beginning of the adsorption step of a two-step cycle, cooling occurs by an interaction between simple waves. The interaction occurs at the bed outlet over a range of times rather than suddenly. Nevertheless, for a cycle with a separate reverse flow cooling step, the interaction occurs at the bed outlet only near the end of the step. Thus, efficient regeneration of the adsorbent near the end of the bed continues during most of the cooling step, thereby extending possibly quite significantly the duration of the ensuing adsorption step. If a separate cooling step is omitted following reverse flow heating, then during the adsorption step the effluent temperature will not at any time increase; rather, it decreases continuously, first quickly and then slowly, over the course of two wave interactions that exist at the bed outlet during most of the step. Furthermore, if heating is with gas containing the adsorbable component, then during the adsorption step the effluent concentration of the adsorbable component also decreases continuously during the two wave interactions prior to the full breakthrough to the feed state, which always occurs as a shock.

This research should help to improve our understanding of nonisothermal adsorption cycles. Continued work in this general area will improve design methods and lead to better energy utilization.

Theory

In this section the mathematical model is developed and simple wave theory is reviewed to the extent necessary to explain the examples. We consider an adsorption cycle with all cycle steps taking place at the same pressure. The adsorbable component is present in an inert carrier gas. Two coupled conservation laws are solved simultaneously, giving two waves (transitions). Each wave may be a simple wave (gradual transition), a shock (abrupt transition), or of combined form. For a cycle step with a nonconstant initial condition, interactions of waves occur. Following our earlier work (Friday and LeVan, 1984), adsorption equilibrium is described by a general relation of the form $c = c(q, T)$.

Material and energy balances

The differential equations for conservation of adsorbate and energy within an isobaric, adiabatic adsorption bed, assuming local equilibrium between stationary and fluid phases and neglecting dispersion, are

$$\rho_b \frac{\partial q}{\partial t} + \epsilon \frac{\partial c}{\partial t} + \epsilon \frac{\partial (vc)}{\partial z} = 0 \tag{1}$$

$$\rho_b \frac{\partial u_s}{\partial t} + \epsilon \frac{\partial (\rho_f u_f)}{\partial t} + \epsilon \frac{\partial (v \rho_f h_f)}{\partial z} = 0 \tag{2}$$

where

$$u_s = (c_s + c_a q)(T - T_{ref}) - \int_0^q \lambda \, dq \tag{3}$$

$$u_f = h_f - P/\rho_f \quad h_f = c_p(T - T_{ref}) \tag{4, 5}$$

Reference states in Eqs. 3 and 5 are adsorbate-free stationary phase at T_{ref} and vapor phase components at T_{ref}. The isosteric heat of desorption λ in Eq. 3 is evaluated at the reference temperature. Also, from Eq. 4, the derivative $\partial(\rho_f u_f)/\partial t$ in Eq. 2 can be replaced by $\partial(\rho_f h_f)/\partial t$.

Dimensionless independent variables and a dimensionless velocity are defined by

$$\tau - \tau' \equiv \frac{\epsilon v_{ref}}{L}(t - t') \tag{6}$$

$$\zeta \equiv \frac{z}{L} \tag{7}$$

$$v^* \equiv \frac{v}{v_{ref}} \tag{8}$$

Primes in Eq. 6 denote values existing at the beginning of a cycle step. Substitution of Eqs. 6, 7, and 8 into Eqs. 1 and 2 gives

$$\rho_b \frac{\partial q}{\partial \tau} + \epsilon \frac{\partial c}{\partial \tau} + \frac{\partial (v^* c)}{\partial \zeta} = 0 \tag{9}$$

$$\rho_b \frac{\partial u_s}{\partial \tau} + \epsilon \frac{\partial (\rho_f h_f)}{\partial \tau} + \frac{\partial (v^* \rho_f h_f)}{\partial \zeta} = 0 \tag{10}$$

We assume that the inert flux at any time is constant throughout the column and that the vapor phase is ideal. This gives for the local interstitial velocity

$$v = v_{inlet} \frac{T}{T_{inlet}} \frac{1 - y_{inlet}}{1 - y} \tag{11}$$

where y is the local vapor phase mole fraction of the adsorbable component. To establish a consistent time scale for the various cycle steps, we let

$$v_{ref} = |v_{inlet}| \frac{T_{ref}}{T_{inlet}} \frac{1 - y_{inlet}}{1 - y_{ref}} \tag{12}$$

In Eqs. 11 and 12, T_{inlet}, y_{inlet}, v_{inlet} (positive or negative), and v_{ref} (positive) may vary among cycle steps; T_{ref} and y_{ref} are constants. Equation 8 now gives simply

$$v^* = \pm \frac{T}{T_{ref}} \frac{1 - y_{ref}}{1 - y} \tag{13}$$

with the sign depending on the flow direction. Furthermore, the value of τ, defined by Eq. 6, is now equal to the number of moles of inert gas passed into the bed since $t = 0$ divided by the number of moles of inert gas contained in one open bed volume at the reference condition. We will elaborate on the advantage of this construction of the τ scale at a later point in connection with the examples.

Matrix formulation and simple waves

Equations 9 and 10 form a reducible quasilinear hyperbolic first-order system. The solution is obtained by a mapping between paths in the hodograph plane (T, q) and characteristic directions in the physical plane (ζ, τ).

To solve for simple waves we adopt a matrix formulation (Jeffrey and Taniuti, 1964; Aris and Amundson, 1973; Jeffrey,

1976; Jacob and Tondeur, 1981, 1983). Equations 9 and 10 are written

$$\overline{\overline{A}}\frac{\partial \bar{Y}}{\partial \tau} + \overline{\overline{B}}\frac{\partial \bar{Y}}{\partial \zeta} = 0 \tag{14}$$

where

$$\bar{Y} \equiv \begin{pmatrix} q \\ T \end{pmatrix} \tag{15}$$

$$\overline{\overline{A}} \equiv \begin{bmatrix} \partial(\rho_b q + \epsilon c)/\partial q & \partial(\rho_b q + \epsilon c)/\partial T \\ \partial(\rho_b u_s + \epsilon \rho_f h_f)/\partial q & \partial(\rho_b u_s + \epsilon \rho_f h_f)/\partial T \end{bmatrix} \tag{16}$$

$$\overline{\overline{B}} \equiv \begin{bmatrix} \partial(v^* c)/\partial q & \partial(v^* c)/\partial T \\ \partial(v^* \rho_f h_f)/\partial q & \partial(v^* \rho_f h_f)/\partial T \end{bmatrix} \tag{17}$$

Equation 14 is premultiplied by the inverse of the $\overline{\overline{B}}$ matrix to give

$$\overline{\overline{C}}\frac{\partial \bar{Y}}{\partial \tau} + \frac{\partial \bar{Y}}{\partial \zeta} = 0 \tag{18}$$

where

$$\overline{\overline{C}} = \overline{\overline{B}}^{-1}\overline{\overline{A}} \tag{19}$$

The two eigenvalues of $\overline{\overline{C}}$ are the local slopes of the characteristics in the physical plane. Letting σ_+ and σ_-, with $|\sigma_+| > |\sigma_-|$, represent the eigenvalues and denoting the corresponding characteristics in the physical plane by C_+ and C_-, we have

$$\frac{d\tau}{d\zeta} = \sigma_+ \text{ along } C_+ \qquad \frac{d\tau}{d\zeta} = \sigma_- \text{ along } C_- \tag{20}$$

The eigenvalues will both have the same sign, positive for positive v_{inlet}. Since the reciprocal of $d\tau/d\zeta$ is a local propagation velocity, C_+ and C_- correspond to the slow and fast waves, respectively.

The loci of pairs of q and T values carried by the C_+ and C_- families in the physical plane are designated Γ_+ and Γ_- in the hodograph plane. Thus, for a pure simple wave, the image of the entire C_+ family lies along a single Γ_+. Values of q and T along a Γ can be determined from the left eigenvectors of $\overline{\overline{C}}$. If we let

$$\bar{\ell}_\pm = (m_\pm, n_\pm) \tag{21}$$

represent the left eigenvectors of $\overline{\overline{C}}$, i.e., satisfying

$$\bar{\ell}_\pm \overline{\overline{C}} = \sigma_\pm \bar{\ell}_\pm \tag{22}$$

then premultiplication of Eq. 18 by $\bar{\ell}_\pm$ gives

$$\bar{\ell}_\pm \left(\sigma_\pm \frac{\partial \bar{Y}}{\partial \tau} + \frac{\partial \bar{Y}}{\partial \zeta}\right) = 0 \tag{23}$$

From Eq. 20, the group in parentheses in Eq. 23 is the derivative $d\bar{Y}/d\zeta$ taken along the $C_\pm$. Thus, Eq. 23 is equivalent to

$$\bar{\ell}_\pm d\bar{Y} = 0 \quad \text{along } C_\pm \tag{24}$$

Since the image of the solution to Eq. 24 lies along a $\Gamma_\pm$ in the hodograph plane, we also have

$$\bar{\ell}_\pm d\bar{Y} = 0 \quad \text{along } \Gamma_\pm \tag{25}$$

which, from Eqs. 15 and 21, is

$$\frac{dq}{dT} = -\frac{n_+}{m_+} \text{ along } \Gamma_+ \qquad \frac{dq}{dT} = -\frac{n_-}{m_-} \text{ along } \Gamma_- \tag{26}$$

Equation 26 depends on variables q and T only and thus can be integrated immediately to establish, once and for all, values of q and T coexisting along Γ in the hodograph plane. The Γ_+ and Γ_- paths will have positive and negative slopes, respectively.

Before proceeding it is important to establish that a Γ_+ (or Γ_-) simple wave region maps into the physical plane giving C_- (or C_+) characteristics that are straight lines along each of which q and T are constant. The argument is as follows (Courant and Friedrichs, 1948). All of the conditions along all of the C_+ characteristics in a Γ_+ simple wave region have their images along a single Γ_+ in the hodograph plane. A Γ_- in this simple wave region intersects this Γ_+ at a single point in the hodograph plane and hence is associated with certain values of q and T. Thus, the C_- characteristics in this Γ_+ simple wave region carry constant values of q and T and from Eq. 20 are straight lines.

Shocks and combined waves

If characteristics rotate in the nonphysical direction in the physical plane, then a shock is formed, with $C_\pm$ characteristics giving rise to an $S_\pm$ shock. The differential equations are then replaced by the difference equations

$$\frac{d\tau}{d\zeta} = \frac{\Delta(\rho_b q + \epsilon c)}{\Delta(v^* c)} = \frac{\Delta(\rho_b u_s + \epsilon \rho_f h_f)}{\Delta(v^* \rho_f h_f)} \tag{27}$$

where the differences are taken between the states on either side of the shock and $d\tau/d\zeta$ is the local slope of the $S_\pm$ shock path in the physical plane. Given one endpoint, Eq. 27 can be solved for two loci of other endpoints in the hodograph plane; the proper path, referred to as $\Sigma_\pm$, is the one tangent to the replaced $\Gamma_\pm$ at the given endpoint.

Combined waves can also occur, including ones with states changing where the simple wave and shock portions join. To solve for these the so-called entropy condition is invoked, which stipulates that the state behind a shock does not propagate slower than the shock and the state ahead of the shock does not propagate faster than the shock. Velocities of respective portions are calculated from Eqs. 20 and 27.

Wave interactions

Our analysis of wave interactions is based on the existence of Riemann invariants for a system of two conservation equations (Courant and Friedrichs, 1948; Jeffrey and Taniuti, 1964; Aris and Amundson, 1973). Although analytical expressions for the Riemann invariants could not be obtained for the problem considered here, their existence nevertheless provides the formal basis for the mapping of wave interactions between hodograph and physical planes.

In all cases presented, the boundary condition for a single

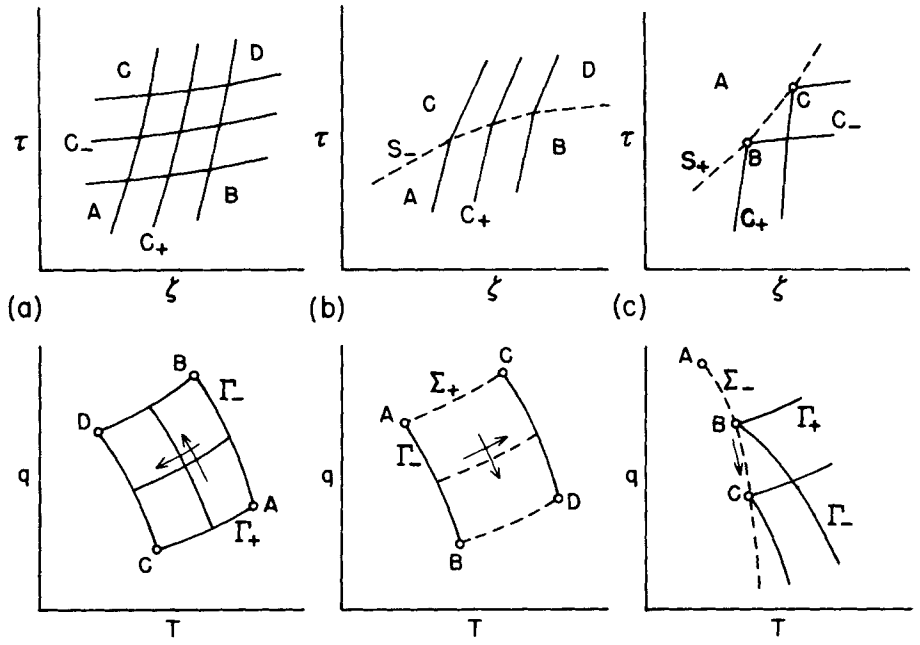

Figure 1. Physical and hodograph planes for wave interactions.

a. Transmission of simple waves
b. Transmission of a simple wave and a shock of different type
c. Absorption of a simple wave by a shock of the same type

cycle step is constant and the initial condition lies along a single Γ_-. The analysis of the resulting wave interactions follows the formal analysis of wave interactions for compressible flow, for which a rigorous proof had been established (Courant and Friedrichs, 1948). Although a rigorous proof of interactions involving shocks for adiabatic adsorption in fixed beds is lacking, we justify our approach by the similarity between the solutions for compressible flow and those for adsorption in fixed beds when regions of constant state are involved. Because the solution space is two-dimensional, the regions of interactions and the paths of the interactions can be obtained unambiguously by knowledge of the adjacent constant states and the paths of the limiting Γ.

Three types of wave interactions will be encountered in the analysis. Sketches of physical and hodograph planes for these are shown in Figure 1. Two other types, the transmission of shocks of different type and the superposition of shocks of the same type, will not occur and are not shown. Wave interactions are discussed only briefly here; they have been considered in detail by Courant and Friedrichs (1948) and Rhee et al. (1970a).

The transmission of two simple waves through one another is shown in Figure 1a. Constant states are represented by A, B, C, and D. We consider a simple wave region containing $AB(\Gamma_-)$ indicated by the family of straight C_+ characteristics. Into this region enters $CA(\Gamma_+)$ with straight C_- characteristics. When interaction begins, the characteristics no longer carry fixed values of q and T; consequently they are no longer straight, signifying changes in propagation velocities. The result of the interaction is to transmit $AB(\Gamma_-)$ to $CD(\Gamma_-)$ and $CA(\Gamma_+)$ to $DB(\Gamma_+)$, with the transmitted waves having straight characteristics. The interaction is followed by knowing that the values of q and T at a point of intersection of C_+ and C_- characteristics in the physical plane are those of the corresponding point of intersection of Γ_+ and Γ_- in the hodograph plane. Since the hodograph plane can be laid out *a priori*, all that is required to analyze this interaction is to establish the characteristic net in the physical plane by mapping points of intersection in the hodograph plane to the physical plane, using Eq. 20 to obtain the local slopes of C_+ and C_-.

The transmission of a simple wave by a shock of different type is shown in Figure 1b. A simple wave region is depicted containing $AB(\Gamma_-)$ into which enters the $CA(\Sigma_+)$ shock with straight shock path S_-. Interaction occurs, deflecting the characteristics and curving the shock path. After interaction is complete, the characteristics and shock path are again straight, with the simple wave having been transmitted to $CD(\Gamma_-)$ and the shock to $DB(\Sigma_+)$. The interaction is analyzed as before, establishing paths in the physical plane by mapping intersections from the hodograph plane. Here, Eqs. 20 and 27 give slopes in the physical plane.

Table 1. System Properties

Physical Properties	
ρ_b	480 kg/m^3
c_s	1.05 kJ/kg · K
c_a	0.140 kJ/mol · K
c_{pa}	1.20 kJ/kg · K
c_{pi}	1.04 kJ/kg · K
λ	43.5 kJ/mol
ϵ	0.4
M_a	0.078 kg/mol
M_i	0.028 kg/mol
Isotherm Parameters	
Q	4.4 mol/kg
K_o	3.88×10^{-8} m^3/mol · K$^{1/2}$
Reference State	
T_{ref}	298 K
y_{ref}	0

The absorption of a simple wave by a shock of the same type is shown in Figure 1c. A Σ_- shock, shown with an endpoint at constant state A, is absorbing a Γ_- simple wave. As interaction occurs the boundary between the shock and simple wave, shown at B then C, moves further from the fixed endpoint. In the physical plane, the C_+ characteristics are absorbed by the S_+ shock path. Although no characteristics are transmitted through the shock path for this case, the C_+ characteristics are transmitted by C_- characteristics, moving the point of intersection of Σ_- and Γ_- along Σ_-. In mapping the solution from the hodograph plane into the physical plane, C_- characteristics are "reflected" from the S_+ shock path to interact with incident C_+ characteristics further downstream, as in Figure 1a. Thus, both the absorption and the continuous transmission of Γ_- are followed simultaneously.

System and Method of Solution

We characterize adsorption equilibria for the benzene-activated carbon-nitrogen system by a Langmuir isotherm, based on the data of James and Phillips (1954), that has been used previously to treat single cycle steps with constant initial and entry conditions (Amundson et al., 1965; Rhee and Amundson, 1970b; Friday and LeVan, 1984). This isotherm is of the form

$$q = \frac{QKc}{1 + Kc} \tag{28}$$

with

$$K = K_0 \sqrt{T} \exp(\lambda/RT) \tag{29}$$

Properties of the system are listed in Table 1. All cycle steps take place at a pressure of 1.0 MPa. The density and heat capacity of the gas phase are calculated assuming ideal gas behavior.

The heating step begins with the bed at a constant initial condition. The solution for this step is developed in the well-established manner (Rhee et al., 1970b), tracing $\Gamma_\pm$ waves from initial and feed states, replacing $\Gamma_\pm$ with $\Sigma_\pm$ when necessary, and checking along $\Sigma_\pm$ for the existence of a combined wave.

Cooling and adsorption steps begin with nonconstant initial conditions. Solutions in regions of the physical plane without wave interactions are determined directly from Eqs. 20 and 27. Wave interactions are calculated by first discretizing the region of interaction in the hodograph plane and solving for the intersections of paths. These points of intersection are then mapped into the physical plane, by rows or columns, beginning with the initial point of intersection. We used second-order numerical schemes for the construction of each plane.

Results

Three examples are considered below:

1. A three-step cycle in which heating and cooling are with solute-free gas in reverse flow
2. A two-step cycle with heating by solute-free gas in reverse flow
3. A two-step cycle with heating by heated feed for the adsorption step in reverse flow

The two-step cycles may in practice be operated as three-step cycles since the adsorption step begins with a cooling interaction. Flow for heating and cooling cycle steps is in the positive ζ direction; flow for adsorption is in the negative ζ direction.

In order to allow comparisons among the various ways of operating the adsorption cycle some parameters are held constant in the examples. The feed temperatures for heating, cooling, and adsorption steps are 373, 298, and 298 K, respectively. The feed for the adsorption step is 10% saturated with benzene, corresponding to a vapor phase concentration of benzene of 0.512 mol/m^3.

In the figures, the sign convention used to label waves should not cause confusion. For example, in a Γ_- simple wave region it is the C_+ characteristics that are the most informative because they carry constant values of q and T and are straight lines. We are interested in the propagation velocities of the states carried by these characteristics. Hence, for regions with no wave interactions symbols of opposite sign are used in hodograph and physical planes.

Example 1

The construction of the solution for heating and cooling with solute-free gas in reverse flow followed by adsorption is shown in Figures 2 and 3, hodograph and physical planes, respectively. Note the changes of scale in Figure 2 at $T = 300$ K and $q = 4$ mol/kg, and in Figure 3 at $\tau = 400$. The saturation capacity of the adsorbent, obtained by substituting the vapor phase concentration of benzene in saturated vapor into Eq. 28, is shown in Figure 2.

The heating step, analyzed first, begins with a uniformly loaded bed at $A(q = 4.12$ mol/kg, $T = 298$ K). At $\tau = 0$, hot nitrogen, corresponding to $B(q = 0, T = 373$ K) is passed into the bed at $\zeta = 0$. Equation 26 is integrated to obtain Γ_+ from A and Γ_- from B. The C_- characteristics fail to rotate properly in the physical plane; thus, the Γ_+ is replaced by Σ_+, obtained from

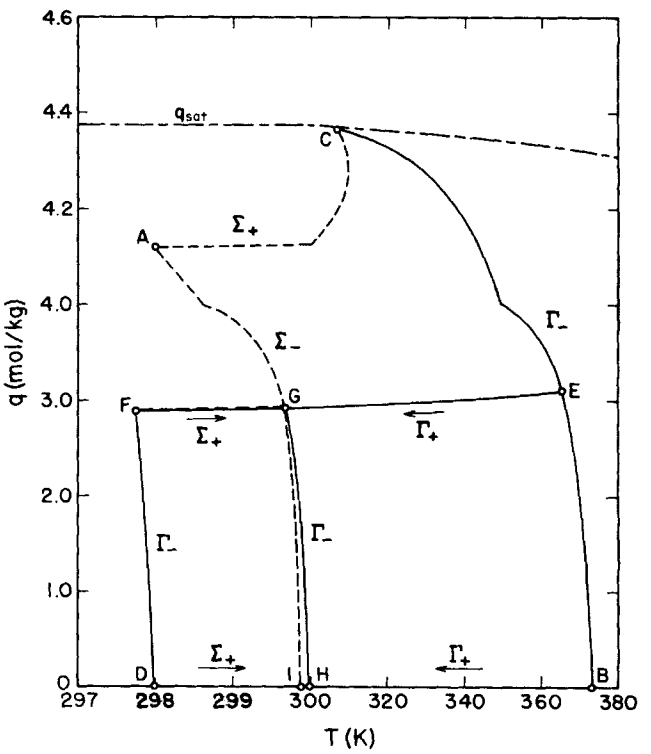

Figure 2. Hodograph plane for example 1.
Note changes of scale at $T = 300$ K and $q = 4$ mol/kg

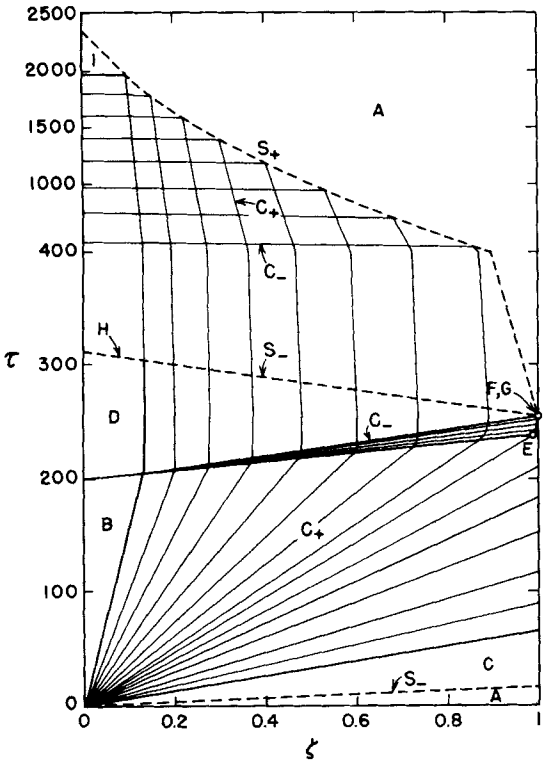

Figure 3. Physical plane for example 1.

Note change of scale at $\tau = 400$. Only representative characteristics are shown. For the adsorption step, characteristics are almost straight, with C_+ carrying almost constant values of q.

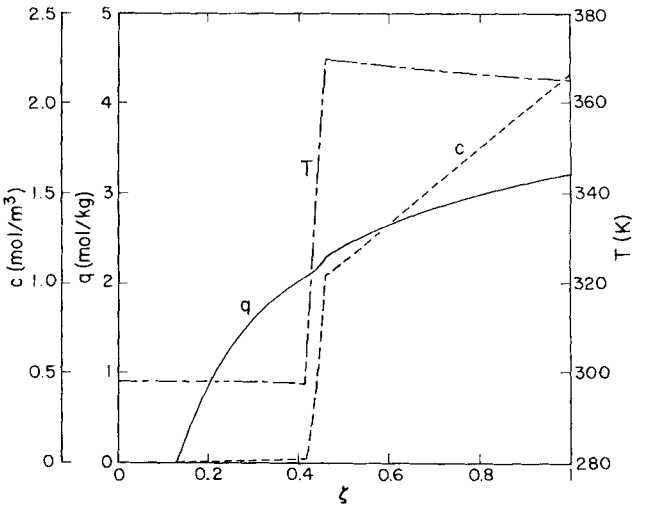

Figure 4. Bed profiles at $\tau = 220$ during cooling step for example 1.

Eq. 27. The solution for the heating step is then $BC(\Gamma_-)$ and $CA(\Sigma_+)$, giving $C(q = 4.36$ mol/kg, $T = 307.0$ K), which is located just below saturation. In the physical plane, the plateau state C is connected to the feed state B by the family of C_+ characteristics and to the initial state A by the S_- shock.

At $\tau = 200$, cool nitrogen corresponding to $D(q = 0$, $T = 298$ K) is passed into the bed at $\zeta = 0$. The solution for this step is constructed by first determining the behavior at the bed inlet, which is initially at B. The points B and D lie on the same Γ_+, giving a pure thermal wave until nonzero concentrations are encountered. (We note here and discuss more fully later that this pure thermal wave is actually a simple wave and not a contact discontinuity, as might be expected, because of the temperature dependence of the fluid phase accumulation term in the energy balance.) Then, C_- characteristics of the cooling wave intersect the C_+ characteristics of the heating wave. Interaction occurs with a portion of the Γ_- from B transmitted along the Γ_+ family to a new Γ_- from D. From the mapping to the physical plane, we find that $BE(\Gamma_-)$ is transmitted to $DF(\Gamma_-)$, giving $F(q = 2.94$ mol/kg, $T = 297.74$ K) and forming the locus of states in the bed at the end of the cooling step, when the last of the C_- characteristics of the interaction has left the bed. The cooling interaction occurs at the bed outlet between $\tau = 245$ and 254. At the end of cooling, the part of the bed containing adsorbate has been cooled to a temperature below that of the cooling gas as the result of supplying energy for desorption. Also, from Figure 3, the cooling wave has markedly reduced rates of wave propagation, as is to be expected.

Figure 4 shows bed profiles at $\tau = 220$, after 20 column volumes of cool gas, measured at the reference temperature, have been passed into the bed for cooling. Between $\zeta = 0$ and 0.13 the adsorbate has been removed entirely and the bed is at D, the feed state. Between $\zeta = 0.13$ and 0.41 the bed is on $DF(\Gamma_-)$. The region of interaction exists between $\zeta = 0.41$ and 0.45. Between $\zeta = 0.45$ and 1.0 the bed is on Γ_- from B to slightly above E.

The adsorption step begins at $\tau = 254$ with the flow direction reversed ($v_{inlet} < 0$) and the condition of the bed lying along $FD(\Gamma_-)$. The feed, added at $\zeta = 1$, is at A. Since the initial condition is on a single Γ_-, propagation begins as a (compressive) simple wave, with Eq. 20 used to determine slopes of the C_+ characteristics in the physical plane. The feed entering the bed at the beginning of the adsorption step encounters the inlet of the bed at F. By considering first simple waves and then shocks, the correct path in the hodograph plane between A and F is found to be $AG(\Sigma_-)$ and $GF(\Sigma_+)$, giving $G(q = 2.95$ mol/kg, $T = 299.68$ K). The solution for the adsorption step is obtained by analyzing the interaction of each of these shocks with the initial Γ_-. The Σ_+, being the fast wave, is considered first and transmits $FD(\Gamma_-)$ to $GH(\Gamma_-)$, as in Figure 1b, giving $H(q = 0$, $T = 299.98$ K). In the physical plane, the interaction of the C_+ characteristics with the S_- shock path is followed until $\tau = 308$, when the shock leaves the bed at $\zeta = 0$. (In order for the entropy condition to be satisfied here, the C_- characteristics immediately above the S_- shock path must intersect the S_- shock path. In this example, however, we have found the C_- and S_- to be very nearly parallel straight lines, and any intersection and resulting interaction has been ignored). The Σ_- in Figure 2, which can be extended to $AI(\Sigma_-)$ establishing $I(q = 0$, $T = 299.92$ K), then absorbs the transmitted Γ_-, as in Figure 1c. Mapping into the physical plane gives the S_+ shock path and states carried by the reflected C_- characteristics as they exit the bed. At $\tau = 1{,}924$, the entire family of C_+ characteristics of the interaction has been absorbed by the S_+ shock path. Shortly thereafter the last of the reflected C_- characteristics leaves the bed, and between then and $\tau = 2{,}310$ pure nitrogen, slightly warmed by the adiabatic adsorption of benzene, leaves the bed at I. The breakthrough at $\tau = 2{,}310$ restores the entire bed to A, the condition at $\tau = 0$. No benzene appears in the effluent at $\zeta = 0$ prior to breakthrough to the feed condition.

Figure 5 shows the bed profiles at $\tau = 700$, well into the

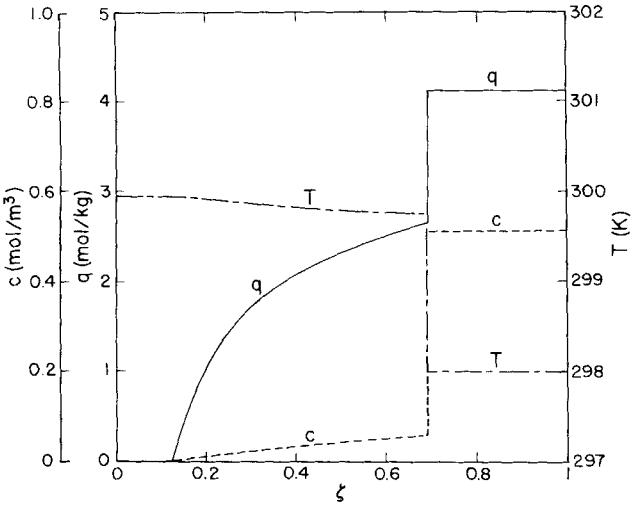

Figure 5. Bed profiles at $\tau = 700$ during adsorption step for example 1.

Note expansion of c and T scales relative to other bed profiles

adsorption step. Flow is from right to left. The S_- shock has passed through the bed. Between $\zeta = 0$ and 0.67 the C_+ characteristics of the transmitted Γ_- are interacting with the C_- characteristics reflected by the upstream S_+ shock, which is located at $\zeta = 0.67$. As time progresses, the effluent temperature slowly decreases as absorption of the C_+ characteristics occurs. The last of the simple wave is overtaken by the shock at $\zeta = 0.10$.

Example 2

The second case considers heating with pure nitrogen in reverse flow followed by adsorption, with omission of a separate

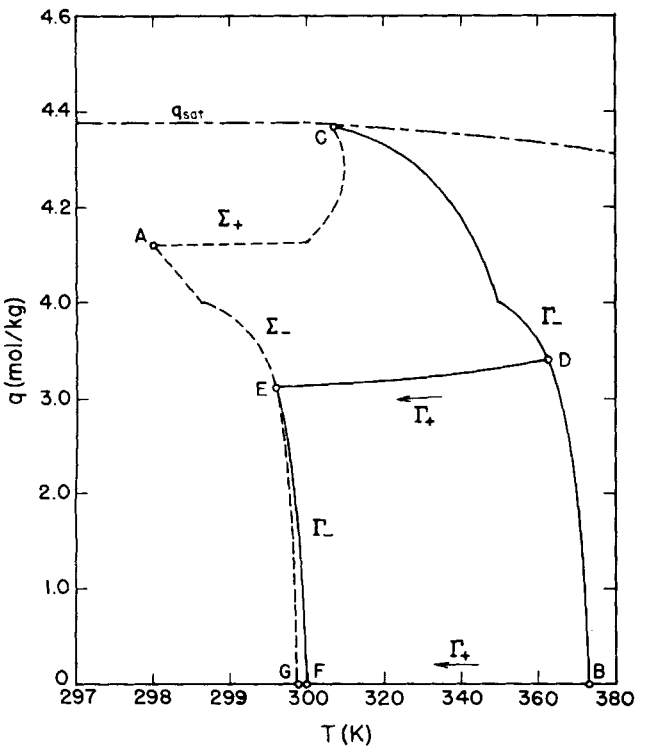

Figure 6. Hodograph plane for example 2.

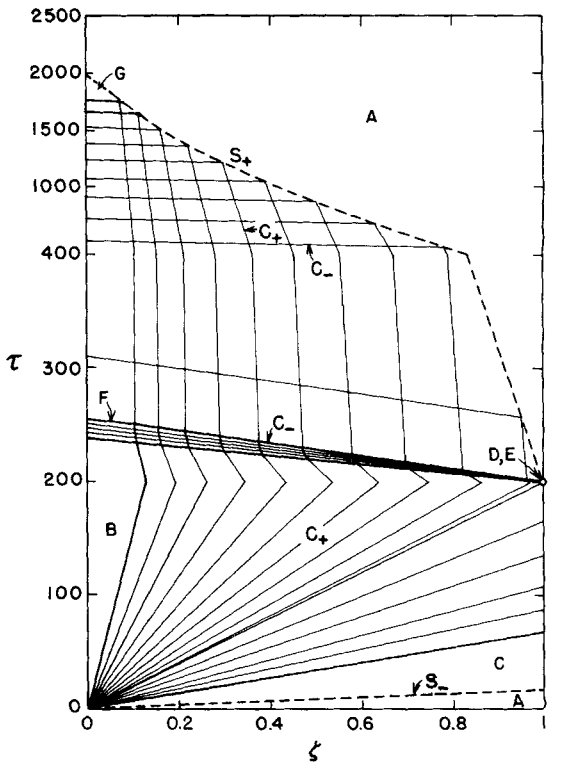

Figure 7. Physical plane for example 2.

cooling step. The possibility of operating a cycle in this mode has been considered in detail by Basmadjian (1975). The solution is constructed in Figures 6 and 7. The initial condition and feed for heating are again the constant states A and B of the previous example. Thus the solution for the heating step is again $BC(\Gamma_-)$ and $CA(\Sigma_+)$.

At $\tau = 200$, the feed for adsorption at state A is introduced at $\zeta = 1$. This cycle step begins with the condition of the bed lying along $DB(\Gamma_-)$ with the bed inlet at $D(q = 3.41$ mol/kg, $T = 361.3$ K). The proper path from A to D is found to be $AE(\Sigma_-)$ and $ED(\Gamma_+)$, giving $E(q = 3.13$ mol/kg,

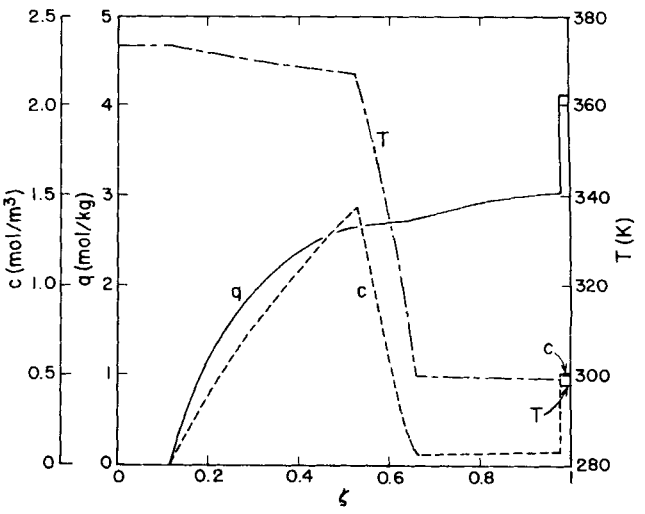

Figure 8. Bed profiles at $\tau = 220$ during adsorption step for example 2.

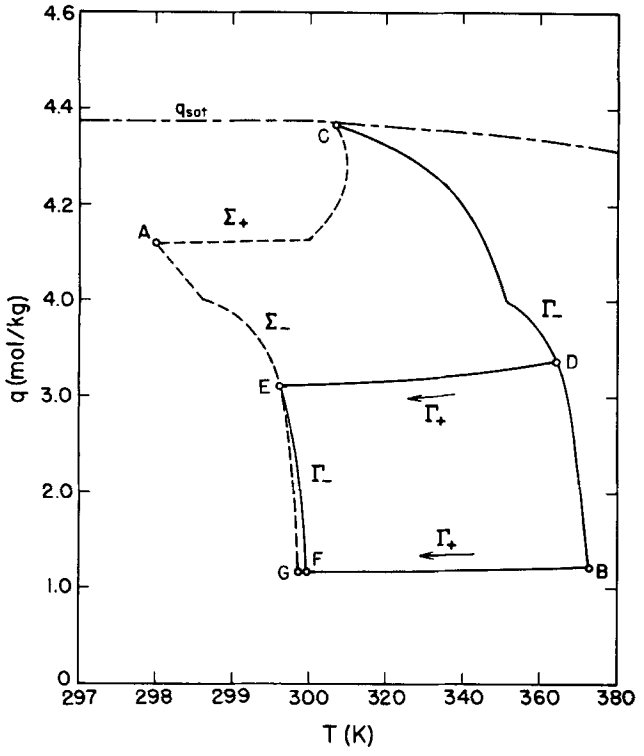

Figure 9. Hodograph plane for example 3.

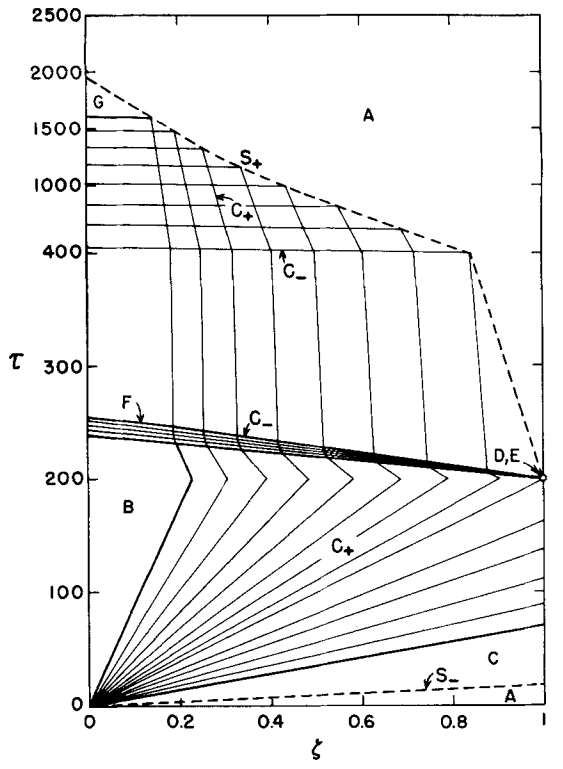

Figure 10. Physical plane for example 3.

T = 299.63 K). The interaction of the Γ_+ with the Γ_- is analyzed first and transmits $DB(\Gamma_-)$ along the Γ_+ family to $EF(\Gamma_-)$, giving $F(q = 0, T = 299.99$ K). The mapping to the physical plane shows that this cooling interaction takes place at the bed outlet at $\zeta = 0$ from $\tau = 243$ to 255. The Σ_- is now extended to $AG(\Sigma_-)$, establishing $G(q = 0, T = 299.92$ K), and absorbs the transmitted Γ_-. The mapping indicates that at τ = 1,727, the shock absorbs the last of the simple wave at $\zeta = 0.07$. Following the quick passage of the last of the reflected C_- characteristics from the bed, the effluent is at state G until breakthrough to the feed state occurs at τ = 1,997. As in the previous example, no benzene is contained in the effluent at $\zeta = 0$ prior to breakthrough.

Bed profiles at $\tau = 220$ for this adsorption step are shown in Figure 8. Flow is from right to left. The bed outlet, between ζ = 0 and 0.12, is at state B, the feed for heating. The Γ_- simple wave from the heating step remains in the bed between $\zeta = 0.12$ and 0.53. The cooling interaction is located from $\zeta = 0.53$ to 0.66. Further upstream, between $\zeta = 0.66$ and 0.98, is the interaction between the incident C_+ and reflected C_- characteristics of the Γ_- absorption by the Σ_- shock, which is located at ζ = 0.98. The bed inlet, from $\zeta = 0.98$ to 1.0, is at state A, the feed for adsorption.

Example 3

Using the feed for the adsorption step heated to 373 K as the feed for heating with reverse flow is the third process variation considered. Only heating and adsorption steps are considered, although in practice the cooling interaction of the adsorption step would usually be treated as a separate step. The solution is constructed in Figures 9 and 10.

The heating step begins with the bed at state A, as in the first two examples. The feed for heating is at $B(q = 1.21$ mol/kg, $T = 373$ K). The solution for the heating step is found to be $BC(\Gamma_-)$ and $CA(\Sigma_+)$, giving $C(q = 4.37$ mol/kg, $T = 306.9$ K).

At $\tau = 200$, the flow direction is reversed and the feed for the adsorption step is passed into the bed at $\zeta = 1$. The condition of the bed initially lies along $DB(\Gamma_-)$ with the inlet at $D(q = 3.37$ mol/kg, $T = 362.8$ K). The correct path from A to D is found to be $AE(\Sigma_-)$ and $ED(\Gamma_+)$, giving $E(q = 3.10$ mol/kg, $T = 299.64$ K). The interactions of the Γ_+ and then the Σ_- with the Γ_- are analyzed as in the previous example, establishing

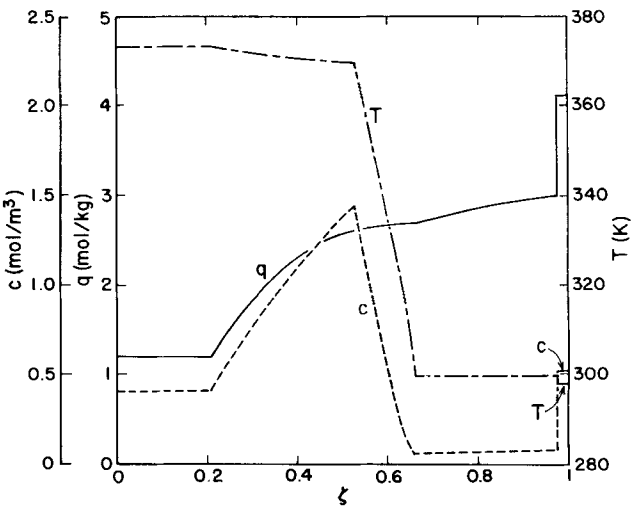

Figure 11. Bed profiles at $\tau = 220$ during adsorption step for example 3.

$F(q = 1.16$ mol/kg, $T = 299.93$ K) and $G(q = 1.16$ mol/kg, $T = 299.87$ K). The cooling interaction occurs at the bed outlet from $\tau = 244$ to 256 and breakthrough to the feed state occurs at $\tau = 1{,}952$. This case differs from the previous ones in that the concentration of benzene in the effluent at $\zeta = 0$ is not zero. Significantly, this concentration never increases prior to breakthrough. From $\tau = 244$ to 1,577, over the course of the two interactions at the bed outlet, it decreases continuously.

Bed profiles at $\tau = 220$ for this example are shown in Figure 11. These differ significantly from those shown in Figure 8 only near the outlet, from $\zeta = 0$ to 0.21, where the bed is at state B. The two interactions, now between $\zeta = 0.52$ and 0.67 and $\zeta = 0.67$ and 0.98, will reduce both T and q at the bed outlet, thereby reducing the effluent concentration.

Discussion

We have treated here cycles taking place at constant pressure. Initial conditions for the cycle steps are constant states or lie along a Γ_-. With pressure changes between cycle steps, the Γ paths in the hodograph plane are altered and nonconstant initial conditions will not lie along a Γ_-. The analysis is still tractable, however, involving initial interactions in all nonconstant state regions. For constant pressure cycles with the development of a liquid phase ($q > q_{sat}$), the analysis is no more difficult than that considered here. The heating step would be treated following Friday and LeVan (1984).

The τ variable defined by Eq. 6 has been chosen to make v^* independent of the values of v_{inlet} for the various cycle steps. Mathematically, this means that the matrices $\overline{\overline{A}}$ and $\overline{\overline{B}}$ and therefore the eigenvalues $\sigma_\pm$ of $\overline{\overline{C}}$ are independent of v_{inlet}. Thus, from Eq. 20, the slopes $d\tau/d\zeta$ retain their magnitudes between cycle steps. Physically, the consequences are that the analysis pertains to cycle steps with different or even varying inlet velocities, and rates of wave propagation are measured in terms of moles of carrier gas fed to the bed rather than by time.

As noted earlier, pure thermal waves in this model can be simple waves or shocks due to a weak temperature dependence of the fluid phase accumulation term in the energy balance. Feeding warm gas into a cool bed results in a shock, while feeding cool gas into a warm bed results in a simple wave. This is due not simply to the change in velocity of the gas, but rather to the temperature dependence of $\rho_f u_f$. Similar behavior, caused by temperature-dependent heat capacities, has been reported by Jacob and Tondeur (1983) and Roizard and Tondeur (1986). Our result pertains to a system with constant heat capacities.

In the examples, temperature changes at the bed outlet due to adiabatic adsorption are modest. The separate cooling step in example 1 gave subcooling of 0.26 K. In all examples, the temperature rise for the adsorption step was about 2 K.

Although no attempt has been made here to determine optimal regeneration conditions in the examples, results for operating the adsorption cycle in the three modes can be compared. The cooling wave in example 1 and the major cooling interactions in examples 2 and 3 each require roughly 55 τ units to pass through the bed, with the interactions existing at the bed outlet for about 10 τ units. The major difference among the cycles from a practical standpoint is the time that the beds can be used effectively for adsorption. In example 1, because benzene continues to be removed from the bed during the cooling step, the adsorption step extends over 2,056 τ units with no loss of benzene. In example 2, the adsorption step lasts 1,797 τ units, or 1,742 τ units after the major cooling interaction has passed from the bed, also with no loss of benzene. In example 3, the effluent from the bed for the adsorption step initially contains benzene at exactly the same mole fraction at which it enters in the feed. Only after the beginning of the cooling interaction at the bed outlet does the bed begin to accumulate benzene. After the completion of the major cooling interaction at the outlet, the bed can be used for adsorption for 1,696 τ units with the effluent containing some benzene. The fact that the effluent contains benzene should tend to prolong the useful time, but this is more than offset by the passage of benzene into the bed during heating and its deleterious effect on regeneration.

Acknowledgment

This research was supported by a grant from the National Science Foundation, No. CBT-8417673.

Notation

c = gas phase concentration of solute, mol/m^3
c_a = heat capacity of adsorbate, kJ/mol · K
c_p = heat capacity of gas phase, kJ/kg · K
c_{pa} = heat capacity of adsorbable component in gas phase, kJ/kg · K
c_{pi} = heat capacity of inert gas, kJ/kg · K
c_s = heat capacity of adsorbent, kJ/kg · K
h_f = enthalpy of gas phase, kJ/kg
K = Langmuir isotherm parameter, m^3/mol
K_o = constant, Eq. 29
L = bed length, m
M_a = molecular weight of adsorbable component, kg/mol
M_i = molecular weight of inert gas, kg/mol
P = total pressure, MPa
q = adsorbed phase concentration, mol/kg
Q = Langmuir isotherm monolayer capacity, mol/kg
R = gas constant
t = time, s
T = temperature, K
u_f = internal energy of gas phase, kJ/kg
u_s = internal energy of stationary phase, kJ/kg
v = interstitial velocity, m/s
v^* = dimensionless velocity
y = mole fraction of adsorbable component in gas phase
z = axial coordinate, m

Greek letters

ϵ = void fraction of packing
ζ = dimensionless axial coordinate
λ = isosteric heat of desorption, kJ/mol
ρ_b = bulk density of packing, kg/m^3
ρ_f = density of gas phase, kg/m^3
τ = dimensionless time

Literature cited

Amundson, N. R., R. Aris, and R. Swanson, "On Simple Exchange Waves in Fixed Beds," *Proc. Roy. Soc.*, **A286,** 129 (1965).

Aris, R., and N. R. Amundson, *Mathematical Methods in Chemical Engineering,* **2,** *First-Order Partial Differential Equations with Applications,* Prentice-Hall, Englewood Cliffs, NJ, 311–316 (1973).

Bailly, M., and D. Tondeur, "Two-Way Chromatography," *Chem. Eng. Sci.*, **36,** 455 (1981).

Basmadjian, D., "On the Possibility of Omitting the Cooling Step in Thermal Gas Adsorption Cycles," *Can. J. Chem. Eng.*, **53,** 234 (1975).

Basmadjian, D., K. D. Ha, and C. Y. Pan, "Nonisothermal Desorption by Gas Purge of Single Solutes in Fixed-Bed Adsorbers. I: Equilibrium Theory," *Ind. Eng. Chem. Process Des. Dev.*, **14,** 328 (1975).

Courant, R., and K. O. Friedrichs, *Supersonic Flow and Shock Waves,* Interscience, New York, 173–204 (1948).

Friday, D. K., and M. D. LeVan, "Thermal Regeneration of Adsorption

Beds: Equilibrium Theory for Solute Condensation," *AIChE J.*, **30**, 679 (1984).
Grevillot, G., D. Tondeur, and J. A. Dodds, "Cyclic Operation of a Fixed-Bed Ion Exchange Column with Three Components," *J. Chromatography*, **102**, 421 (1974).
Helfferich, F., and G. Klein, *Multicomponent Chromatography*, Dekker, New York, 105–272 (1970).
Jacob, P., and D. Tondeur, "Nonisothermal Gas Adsorption in Fixed Beds. I: A Simplistic Linearized Equilibrium Model," *Chem. Eng. J.*, **22**, 187 (1981).
———, "Nonisothermal Gas Adsorption in Fixed Beds. II: Nonlinear Equilibrium Theory and 'Guillotine' Effect," *Chem. Eng. J.*, **26**, 41 (1983).
James, D. H., and G. S. G. Phillips, "The Chromatography of Gases and Vapors. III: The Determination of Adsorption Isotherms," *J. Chem. Soc.*, **1954**, 1066 (1954).
Jeffrey, A., *Quasilinear Hyperbolic Systems and Waves*, Pitman, London, 42–164 (1976).
Jeffrey, A., and T. Taniuti, *Nonlinear Wave Propagation*, Academic Press, New York, 65–135 (1964).
Klein, G., M. Nassiri, and J. M. Vislocky, "Multicomponent Fixed-Bed Sorption with Variable Initial and Feed Compositions. Computer Prediction of Local Equilibrium Behavior," *Adsorption and Ion Exchange-Progress and Future Prospects*, J. D. Sherman and T. Vermeulen, Eds., *AIChE Symp. Ser. No. 233*, **80**, 14 (1984).
Knaebel, K. S., and R. L. Pigford, "Equilibrium and Dissipative Effects in Cycling Zone Adsorption," *Ind. Eng. Chem. Fundam.*, **22**, 336 (1983).
Lax, P. D., "Weak Solutions of Nonlinear Hyperbolic Equations and Their Numerical Computation," *Comm. Pure Appl. Math.*, **7**, 159 (1954).
———, "Hyperbolic Systems of Conservation Laws. II," *Comm. Pure Appl. Math.*, **10**, 537 (1957).
Pan, C. Y., and D. Basmadjian, "An Analysis of Adiabatic Sorption of Single Solutes in Fixed Beds: Pure Thermal Wave Formation and Its Practical Implications," *Chem. Eng. Sci.*, **25**, 1653 (1970).
———, "An Analysis of Adiabatic Sorption of Single Solutes in Fixed Beds: Equilibrium Theory," *Chem. Eng. Sci.*, **26**, 45 (1971).
Rhee, H. K., and N. R. Amundson, "An Analysis of an Adiabatic Adsorption Column. I: Theoretical Development," *Chem. Eng. J.*, **1**, 241 (1970).
———, "Analysis of Multicomponent Separation by Displacement Development," *AIChE J.*, **28**, 423 (1982).
Rhee, H. K., R. Aris, and N. R. Amundson, "On the Theory of Multicomponent Chromatography," *Phil. Trans. Roy. Soc.*, **A267**, 419 (1970a).
Rhee, H. K., E. D. Heerdt, and N. R. Amundson, "Analysis of an Adiabatic Adsorption Column. II: Adiabatic Adsorption of a Single Solute," *Chem. Eng. J.*, **1**, 279 (1970b).
Roizard, C., and D. Tondeur, "Heat Transfer in Percolated Fixed Beds with Temperature-Dependent Physical Properties—Compressive and Dispersive Effects," *Int. J. Heat Mass Transfer*, **29**, 1021 (1986).

Manuscript received Mar. 28, 1986, and revision received Sept. 27, 1986.